Dissolution in (1+1) dimensions: a numerical study

LETTER TO THE EDITOR

Dissolution in (1+1) dimensions: a numerical study

G Poupart and G Zumofen

Laboratorium für physikalische Chemie, ETH-Zentrum, CH-8092 Zürich, Switzerland

Abstract. We study by numerical simulations the growing interfaces due to dissolution in $d = (1 + 1)$ dimensions. We consider a model based on simple, temperature-dependent microscopic dissolution rules, and we investigate the scaling properties of the growing surface structure. The roughness exponent α and the dynamical scaling exponent β are determined for various temperatures. We report on a complicated temperature dependence of the exponent β which for three particular temperatures approaches theoretical limiting values. Also studied is the average nearest-neighbour height difference which follows a linear temperature dependence at saturation.

1. Introduction

The problem of surface or interface growth far from equilibrium has received considerable attention over the last few years [1–3]. Many growth models have been introduced to study the morphology of growing surfaces, e.g. the Eden model, ballistic and random deposition, both as lattice and off-lattice models, with and without rearrangement of the particle positions [4, 5]. The interest in these models is due to their role played in the understanding of crystal and thin-film growth processes and of interface dynamics in random media. Futhermore, these models are of interest because of the intimate relationship between surface growth and directed polymers [6, 7] and the particle density evolution in reaction dynamics [8, 9]. Also, the resulting surfaces exhibit fractal characteristics, most of them being *self-affine* [10].

The surface roughness is the property which has been predominantly investigated. Usually the roughness is defined as the width (or variance) $\xi(t)$ which for a one-dimensional substrate is calculated as

$$\xi(t)^2 = \frac{1}{L}\left\langle \sum_{i=1}^{L}[h(i,t) - \overline{h(t)}]^2 \right\rangle \tag{1}$$

where $h(i,t)$ is the height of the surface at location i at time t; L is the size of the one-dimensional substrate. $\overline{h(t)}$ denotes the mean height at time t for a particular surface configuration and the average in (1) is taken over all possible configurations. Note that this definition of roughness ignores overhangs.

Starting from a flat surface, the time evolution of the width is as follows. The width first grows as a power law with the dynamical exponent β. At longer times, the

width shows a crossover and saturates at long times, reaching a value which depends on the substrate as $\xi \sim L^\alpha$ where α denotes the roughness exponent. The behaviours, characteristic for the two temporal regimes, can be recast in a single scaling form [11]

$$\xi(t) = L^\alpha f(t/L^z)$$

where z is given by $z = \alpha/\beta$. $f(x)$ denotes the scaling function

$$f(x) \sim \begin{cases} x^\beta & x \ll 1 \\ \text{constant} & x \gg 1. \end{cases} \tag{2}$$

The analytic treatment of growth and deposition processes was initiated by Edwards and Wilkinson [12] who derived a linear Langevin equation for the description of surface growth. From their work the values for the two characteristic exponents in $d = (1+1)$ dimensions are $\alpha = \frac{1}{2}$, $\beta = \frac{1}{4}$. Later this equation was extended by Kardar *et al* who proposed the following nonlinear equation for surface growth (KPZ equation) [13]:

$$\frac{\partial \bar{h}}{\partial t} = \nu \nabla^2 \bar{h} + \frac{\lambda}{2}(\nabla \bar{h})^2 + \eta(x,t). \tag{3}$$

Here $\bar{h}(x,t)$ measures the height of the surface relative to the average height. The diffusion term on the right-hand side of (3) describes the relaxation due to the surface tension ν. The nonlinear term was introduced to account for the lateral growth. $\eta(x,t)$ denotes a fluctuation term which is usually assumed to be delta-correlated in space and time (white noise). For the KPZ equation it has been found that the dynamical and roughness exponents are related to each other by the following scaling relationship [13,14]:

$$\alpha + \alpha/\beta = 2. \tag{4}$$

For a one-dimensional substrate the exponents are $\alpha = \frac{1}{2}$ and $\beta = \frac{1}{3}$. Based on the KPZ equation two limiting cases can be discussed: if the nonlinear term is omitted, $\lambda = 0$, (3) reduces to the linear Langevin equation treated by Edwards and Wilkinson and thus $\alpha = \frac{1}{2}$ and $\beta = \frac{1}{4}$. If the diffusion term is also dropped, $\lambda = \nu = 0$, and the random deposition model emerges. In this case there is no relaxation and thus there is also no saturation; therefore only the dynamical exponent is of importance which is trivially $\beta = \frac{1}{2}$.

In this letter we present the dissolution model which was introduced in a different context by Wehrli [15] to describe the interdependence of the surface morphology and the dissolution kinetics of minerals. In this model particles are removed from the surface according to dissolution probabilities. Re-absorption is ignored, corresponding to the situation of low chemical potential. The dissolution probabilities are assumed to depend on the local surface structure and to be activated, i.e. they depend on the temperature. In turn the temperature is a parameter which allows one to tune the characteristics of the dissolution process and to study the roughness depending on parametrized microscopic dissolution rules.

2. The model and simulation results

The dissolution model is based on rates at which particles dissolve from the surface. These rates are assumed to depend on the local structure as follows:

$$k_n = \kappa \exp(-n\omega) \qquad (5)$$

where n denotes the number of nearest neighbours for a particular lattice site. For the one-dimensional substrate, n may take one of the following possible values: $n = 1, 2, 3$. The model is assumed to follow the solid-on-solid condition, i.e. overhangs are ignored. κ is a dissolution rate and ω is the dimensionless activation enthalpy for which we make the identification $\omega = 1/T$, where T is the reduced (dimensionless) temperature.

The simulation calculation starts from a flat surface for given lattice size L and temperature T. A site j is chosen at random and the number n of nearest neighbours of this site is determined. Then the height h_j is decremented according to the probability

$$p_n(h_j \rightarrow h_j - 1) \sim \exp(-n/T). \qquad (6)$$

In all cases periodic boundary conditions are imposed on the heights. The process is repeated and the surface is analysed in time intervals which are measured in terms of dissolved layers or, more precisely, time is set to $t = \overline{\Delta h}$, where $\overline{\Delta h}$ denotes the number of dissolved layers. This definition is chosen for convenience to present the results on equal scales independent of the parameters κ, L, T. The number of trial events (proportional to CPU-time) and $\overline{\Delta h}$ are linearly related except for very short times in the beginning of the simulation for which a transient nonlinear relationship is observed.

We report on results obtained for temperatures which were varied in the range $0.4 \leqslant T \leqslant 100$. We begin with the short-time behaviour for which our system was as large as $L = 2^{14}$; this size was necessary to avoid finite-size effects and to obtain reliable exponents at low temperatures, $T \leqslant 1$. For higher temperatures, $T \geqslant 1$, smaller lattice sizes led to satisfactory results. In most cases we followed the evolution up to times $t = 4000$, measured in numbers of dissolved layers, and averages were taken typically over 50 independent realizations.

In figure 1 we present the surface width $\xi(t, T)$ obtained from the simulation calculations for various temperatures. The widths given by full lines are plotted on log–log scales. The slopes obtained from a fit in the range $1000 \leqslant t \leqslant 4000$ are indicated by broken lines. For the low- and the high-temperature limits the theoretical slopes of $\frac{1}{3}$ and $\frac{1}{2}$, respectively, are given as chain lines. The figure demonstrates that the widths converge rather slowly to the expected scaling behaviour. For low temperatures, $T \leqslant 1.0$, we observe a convex behaviour while for high temperatures, $T \geqslant 1.5$, the curves show a concave characteristic which is explained as follows. For high temperatures, on the one hand, the three p_n values are almost identical. Therefore, at short times the situation resembles that observed in random deposition for which $\beta = \frac{1}{2}$ holds. At later times the differences between the p_ns become crucial so that the relaxation of the surface slows down the growth of the surface width. For low temperatures, on the other hand, due to the big differences between the three
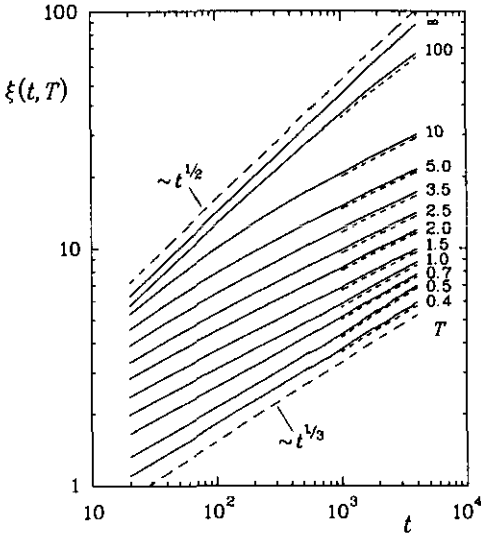
Figure 1. The surface width $\xi(t,T)$ as a function of time for various temperatures T as indicated at the right margin. For $T = \infty$ the random deposition (dissolution) results are depicted. The sample length was $L = 2^{14}$ and averages were taken over 50 runs. The broken lines denote the fitted slopes. For comparison, the power-law behaviours with exponents $\beta = \frac{1}{2}$ and $\frac{1}{3}$, respectively, are also shown. Note that the different lines are shifted to avoid overlap.
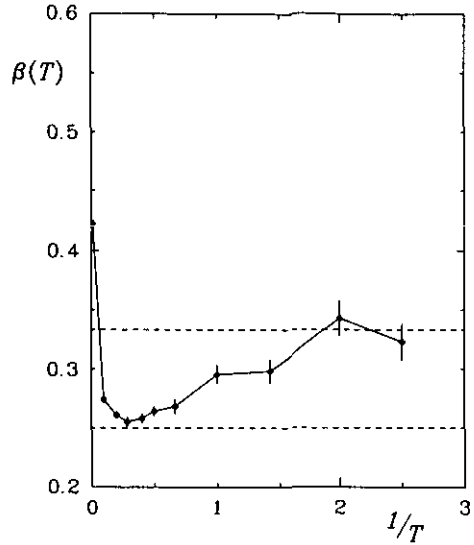
Figure 2. The dynamical scaling exponent $\beta(T)$ as a function of the inverse temperature and the sample length L. For $L = 16\,384$, data are taken from figure 1. The full curve serves as a guide to the eye. The broken lines indicate the limiting low-temperature behaviour of $\frac{1}{3}$ and the Edwards–Wilkinson value of $\frac{1}{4}$.

p_ns the growth accelerates with increasing time since the structured surface facilitates the dissolution process.

The values of the dynamic exponent $\beta(T)$ obtained from the fitting are presented in table 1 and are also plotted in figure 2 as a function of the inverse temperature $1/T$ for different system sizes. With decreasing temperature the exponent beginning at a value of $\beta = 0.42$ for $T = 100$ decreases and reaches a minimum at $T_c \simeq 3.5$ where β takes a value of $\beta \simeq \frac{1}{4}$. Then the exponent increases and saturates for small temperatures at a value of $\beta \simeq \frac{1}{3}$. This behaviour is a characteristic of our simulation results and is independent of the system size L which was varied in the range of $2048 \leqslant L \leqslant 16\,384$.

From these findings one is tempted to conjecture that asymptotically, for $L \to \infty$, the dynamical exponent takes three values: $\beta = \frac{1}{2}$ for $T = \infty$, $\beta = \frac{1}{4}$ for $\infty > T > T_c$, and $\beta = \frac{1}{3}$ for $T_c > T$, i.e. as a function of temperature, β shows sharp transitions at $T = \infty$ and $T = T_c$. The smooth variation of β between the three limiting values observed in the simulation results would then be a consequence of the finite system size imposed by computer limitations.

In the light of this conjecture we analysed $\xi(t,T)$ paying particular attention to its asymptotic behaviour. In fact, for high temperatures, $T > T_c$, $\xi(t,T)$ shows very slow convergence to its asymptotic power-law behaviour. This finding is clearly in favour of

Table 1. The dynamical exponent $\beta(T)$ obtained from a fit to the width $\xi(t, T)$ and $\alpha + \alpha/\beta$ with $\alpha = 0.5$; see text for details.

T	β	$\alpha + \alpha/\beta$
0.4	0.32	2.05
0.5	0.34	1.96
0.7	0.30	2.18
1.0	0.30	2.19
1.5	0.27	2.37
2.0	0.26	2.40
2.5	0.26	2.44
3.5	0.26	2.46
5.0	0.26	2.42
10.0	0.27	2.33
100.0	0.42	1.69

the conjecture that $\beta = \frac{1}{4}$ in this temperature regime. We also performed simulation calculations up to very long times. For $T = 20$, $L = 4096$ and $t_{max} = 100\,000$ the fitted exponent was $\beta \simeq \frac{1}{4}$, without any indication that the behaviour was influenced by the crossover to saturation.

For low temperatures, $T < T_c$, the simulation results are more conclusive. As a function of time $\xi(t, T)$ quickly reaches the asymptotic power-law behaviour and our results indicate a smooth variation of the exponent for $T < T_c$. Nevertheless, we cannot rule out the possibility that $\xi(t, T)$ converges extremely slowly and that β has a sharp transition at T_c.

We point out that transitions between discrete values of β were also observed for other growth models. Krug [16] investigated the PNG model and observed that $\beta = \frac{1}{3}$ except in a particular symmetric case for which $\beta = \frac{1}{4}$. Furthermore, Family [17] found that the introduction of relaxation in the random deposition model causes the exponent β to drop sharply from $\frac{1}{2}$ to $\frac{1}{4}$.

We continue by reporting on the roughness exponent α which we obtained using the L-dependent saturation values of the surface width. We also considered the small j-behaviour of the height-difference correlation function $G(j, t) = \langle [h(j, t) - h(0, t)]^2 \rangle$ which scales as $j^{2\alpha}$ for small j. We found that within the numerical accuracy the roughness exponent was $\alpha \simeq \frac{1}{2}$ irrespective of the temperature. The first method proved to be more involved because of significant fluctuations in the saturation widths and the long times required to reach saturation, while the results based on the height-difference correlation function turned out to be more reliable.

With regard to the scaling relationship (4) we also present the sum $\alpha + \alpha/\beta$ in table 1. The sum takes values of approximately 2 at low temperatures, increases smoothly, and almost reaches values of 2.5 for $T \geqslant T_c$. For $T = 100$ the value of 1.69 indicates that the conditions are close to those of the random-deposition model for which the roughness exponent is meaningless. Nevertheless, the tendency is obvious and is analogous to the results obtained for β. For low temperatures, $T < T_c$, the KPZ equation applies, so that $\alpha + \alpha/\beta = 2$, while for high temperatures, $T > T_c$, the Edwards–Wilkinson picture is appropriate with $\alpha = \frac{1}{2}$ and $\beta = \frac{1}{4}$ so that

$\alpha + \alpha/\beta = 2.5$. The smooth transition between the two discrete values corresponds to that obtained for β in the same temperature range.

Making use of these exponents and of the scaling relationship, equation (2), we are able to collect the width results in a master plot. This is demonstrated in figure 3 where the rescaled widths ξ/L^{α} are plotted versus the rescaled time $t/L^{\alpha/\beta}$ for various lattice sizes and for the temperature $T = 0.4$. We observe a pronounced data collapse onto a single scaling curve which follows the expected power-law increase for short times with a crossover to saturation close to $t/L^{\alpha/\beta} = 0.05$. This scaling behaviour was obtained independently of the chosen temperature.
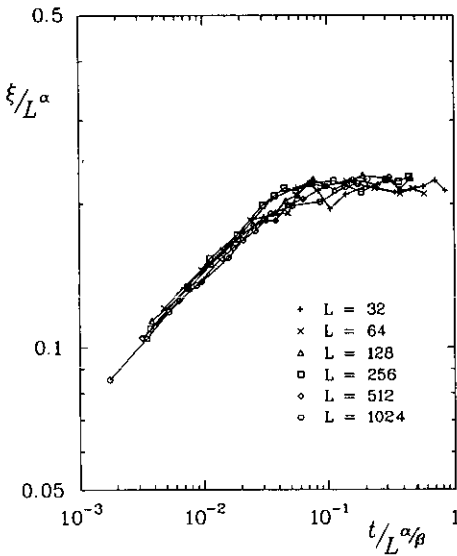

Figure 3. Saturation effect in the dissolution model. Plotted are the rescaled widths versus the rescaled time for various system sizes as indicated. The temperature considered is $T = 0.4$.
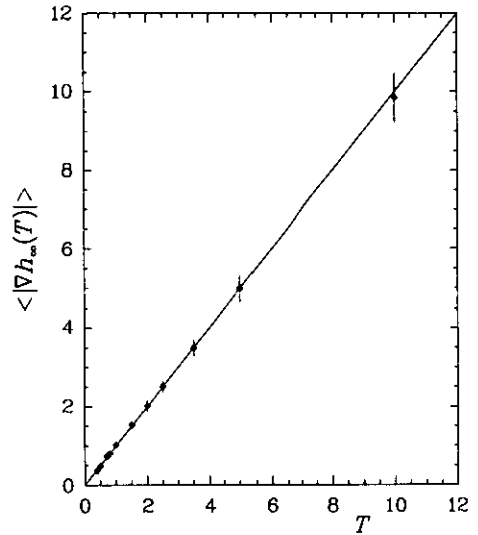
Figure 4. The mean-nearest-neighbour differences $\langle |\nabla h_{\infty}(T)| \rangle$ as a function of the temperature. The standard deviations are indicated by vertical error bars. The sample length was $L = 256$ and averages were taken over 50 runs.

We analysed other quantities relevant to the description of the surfaces such as the average nearest-neighbour differences $\langle |\nabla h| \rangle$ and the step densities. Here we present results on $\langle |\nabla h| \rangle$. This quantity is found to saturate at a value $\langle |\nabla h_{\infty}(T)| \rangle$ which depends only on the temperature T, irrespective of the sample length L. Remarkably, the saturation value obeys a simple linear relationship: $\langle |\nabla h_{\infty}(T)| \rangle = T$ which is evident from figure 4. Wehrli [15] reported the same finding for his simulations in $d = (2 + 1)$ dimensions.

In this letter we concentrated on the analysis of the scaling properties of the surface growth for the dissolution model. Our results follow the scaling relationship presented in equation (2). The dynamical exponent β shows an interesting temperature dependence approaching the three limiting cases mentioned in the introduction: for infinite temperature the local structure has no importance for the dissolution probability and the system follows the random deposition (dissolution)

process with the exponent being $\beta(T \rightarrow \infty) \simeq \frac{1}{2}$. For intermediate temperatures the probabilities p_n are such that the relaxation is strong compared with the lateral growth. Thus in this temperature regime the model is close to the Edwards–Wilkinson assumption and correspondingly $\beta \simeq \frac{1}{4}$. We point out that this value is outstanding for a growth model without restructuring: such low values are usually reached only for models for which restructuring is allowed [17–19]. Finally, for very low temperatures, the microscopic growth probabilities are such that lateral growth is as important as relaxation. Thus the KPZ equation applies and $\beta \simeq \frac{1}{3}$. Similarly the sum rule (4) holds when $\beta \simeq \frac{1}{3}$, but with increasing temperature there is a transition and the sum $\alpha + \alpha/\beta$ reaches the value of 2.5 which is correct for the Edwards–Wilkinson assumption.

In conclusion, depending on temperature, we observe a transition between different kinetic phases. This is reminiscent of some recently reported results for models which also include tunable parameters [20]. Further investigations are necessary to attain a profound understanding of the scaling properties characteristic for the dissolution model in $d = (1 + 1)$ and higher dimensions.

References

[1] H E and Stanley N Ostrowsky (ed) 1986 *On Growth and Form* (Boston: Martinus Nijhoff)
[2] H E and Stanley N Ostrowsky (ed) 1987 *Random Fluctuations and Pattern Growth: Experiments and Models* (Dordrecht: Kluwer)
[3] Vicsek T 1989 *Fractal Growth Phenomena* (Singapore: World Scientific)
[4] Meakin P 1987 *CRC Crit. Rev. Solid State Mater. Sci.* **13** 143
[5] Family F 1990 *Physica* **168A** 561
[6] Kardar M and Zhang Y-C 1987 *Phys. Rev. Lett.* **58** 2087
[7] Zumofen G, Klafter J and Blumen A 1992 *Phys. Rev.* A **45** 7624
[8] Zhang Y-C 1987 *Phys. Rev. Lett.* **59** 1276
[9] Zumofen G, Klafter J and Blumen A 1992 *Phys. Rev.* A **45** 8977
[10] Mandelbrot Benoit B 1977 *The Fractal Geometry of Nature* (San Francisco: Freeman)
[11] Family F and Vicsek T 1985 *J. Phys. A: Math. Gen.* **18** L75
[12] Edwards S F and Wilkinson D R 1982 *Proc. R. Soc.* A **381** 17
[13] Kardar M, Parisi G and Zhang Y-C 1986 *Phys. Rev. Lett.* **56** 889
[14] Krug J 1987 *Phys. Rev.* A **36** 5465
[15] Wehrli B 1989 *J. Coll. Interf. Sci.* **132** 230
[16] Krug J 1990 *Die Entstehung fraktaler Oberflächen* Reihe Physik (Frankfurt: Harri Deutsch)
[17] Family F 1986 *J. Phys.* A **19** L441
[18] Meakin P and Jullien R 1987 *J. Physique* **48** 1651
[19] Meakin P and Jullien R 1989 *Europhys. Lett.* **9** 71
[20] Phillips R and Chrzan D C 1991 *Phys. Rev. Lett.* **67** 220